Mini-UAV-Borne LIDAR for Fine-Scale Mapping

Yi Lin, Juha Hyyppä, and Anttoni Jaakkola

***Abstract*—Light detection and ranging (LIDAR) systems based on unmanned aerial vehicles (UAVs) recently are in rapid advancement, while mini-UAV-borne laser scanning has few reported progress, notwithstanding so extensively required. This study established a pioneered mini-UAV-borne LIDAR system—Sensei, schematically with an Ibeo Lux scanner mounted on a small Align T-Rex 600E helicopter. Furthermore, the associated data processing involved in the coordinate triple, pulse intensity, and multiechoes per pulse was explored to validate its applicability for fine-scale mapping, in terms of, e.g., tree height estimation, pole detection, road extraction, and digital terrain model refinement. The feasibility and advantages of mini-UAV-borne LIDAR have been demonstrated by the promising results based on the real-measured data.**

***Index Terms*—Fine scale, light detection and ranging (LIDAR), mapping, mini-unmanned aerial vehicle (UAV).**

I. Introduction

As THE state-of-the-art mapping technology, light detection and ranging (LIDAR) recently has been developing quickly, which can depict targets through the associated collections of spatially distributed points with accurate coordinate triples. In particular, airborne LIDAR has been extensively explored and also employed in a variety of remote sensing applications, e.g., building segmentation [1], defoliation investigation [2], forest biomass inventory [3], and tree structural parameter retrieval [4]. Among these topics, higher sampling density is commonly expected as a premier to better represent the characteristics of objects.

The current airborne LIDAR systems, however, mostly sample laser hits in a limited density. Particularly in the monitoring of large areas, it was revealed that it is economically unfeasible to map data with classic scanning systems of more than one laser pulse per square meter [5]. Therefore, some local data collected in fine scales are at least required as the reference for revising the traditional LIDAR-derived results. Mobile laser scanning (MLS) as a settlement can offer this kind of data [6], [7], but for dense forests, MLS suffers from the issue of no entry. Moreover, the scanning angles of MLS and airborne LIDAR systems are not consistent. Hence, an efficient, accurate, low-cost, and flexible surveying scheme with the same scanning view is needed to overcome this problem.

Unmanned aerial vehicles (UAVs) as alternative platforms for laser scanning provide a good choice to overcome the aforementioned issue. UAVs have been utilized for remote sensing, and the preliminary schematics and prototypes of UAV-borne LIDAR systems, or even more comprehensive systems, have also been constructed. Johnson discussed the configurative designs of UAV-based laser scanning [8], and Nagai *et al.* established a UAV-borne integration system with a Sick laser scanner, charge-coupled device (CCD) cameras, inertial measurement unit (IMU), and GPS [9]. However, the UAVs referred in [8] and [9] are large (the helicopter UAV used in [9] weighs 330 kg), and this is not appropriate for some special application contexts, e.g., the UAV-borne LIDARs need to be manually carried into deep forests for investigation of the key plots.

Mini-UAVs seem to be a natural choice as the supplementary solution. Installed with IMU and GPS, mini-UAV-borne LIDAR systems can act further as a promising mapping plan, which can deploy efficient, accurate, and flexible surveying projects. In some countries, the use of lightweight mini-UAV systems is not as strictly regulated as the flight of heavier UAVs, which makes mini-UAV-associated applications substantially easier. However, the utilization of mini-UAV for laser scanning is still a new research domain, and almost no integral efforts have been reported. A remotely controlled helicopter installed with GPS navigation sensors and a laser range finder or altimeter for topographic surveys was depicted in [10]. Moreover, a miniature laser range finder/altimeter has been developed for autonomous navigation and landing in small UAVs [11], and the mini-UAV optical images were also tried to combine with laser scanning performed on the conventional platforms [12]. From literature review, it can be learned that mini-UAVs have not yet been used for detailed surveying and modeling of objects.

This letter presents a pioneered complete mini-UAV-borne LIDAR system—Sensei, which is newly developed in the Finnish Geodetic Institute, and the associated data processing involved in coordinate triple, pulse intensity, and multiechoes per pulse is explored for testing its applicability for fine-scale mapping. Based on the real-measured point clouds, the advantages of mini-UAV-borne LIDAR are revealed in terms of, e.g., tree height estimation, pole detection, road extraction, and digital terrain model (DTM) refinement. Moreover, the flexibility of Sensei system, which can be installed on the top of a vehicle as an MLS system, is also discussed.

II. Materials

A. Sensei System

In the configuration of mini-UAV-borne Sensei system, the instruments are mounted under a radio-controlled helicopter, as shown in Fig. 1. The airframe used is Align T-Rex 600E, modified to utilize up to 710-mm main rotor blades and fitted with a 4.2-kW electric motor. The sensor frame is isolated from the airframe to absorb high-frequency vibrations. The Sensei

Manuscript received August 6, 2010; revised August 26, 2010 and September 7, 2010; accepted September 13, 2010. Date of publication November 8, 2010; date of current version April 22, 2011. This work was supported in part by the Academy of Finland under Grant 129489.

The authors are with the Department of Remote Sensing and Photogrammetry, Finnish Geodetic Institute, 02431 Masala, Finland (e-mail: yi.lin@fgi.fi).

Digital Object Identifier 10.1109/LGRS.2010.2079913

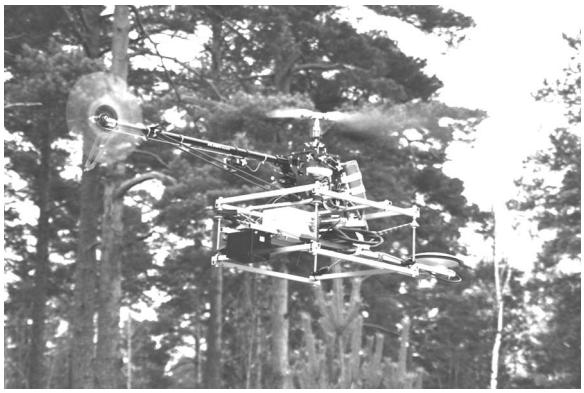

Fig. 1. Demonstration of the mini-UAV-borne Sensei system.

TABLE I
WEIGHTS OF THE SYSTEM COMPONENTS (INCLUDING CABLES)

Component	Weight [Kg]	Component	Weight [Kg]
GPS/IMU	2.5	GPS antenna	0.7
Laser scanner (Ibeo)	1.2	Laser scanner (Sick)	1.6
CCD camera	0.7	Spectrometer	0.7
Thermal camera	0.6	Computer	1.3
Sensor battery	0.4	Sensor frame	1.5
Synchronization box	0.2		

system was originally designed to comprise two different laser scanners, namely, Ibeo Lux and Sick; an AVT Pike F-421C CCD camera; a Specim V10H spectrometer; a NovAtel SPAN-CPT tightly coupled GPS/INS positioning system; and a Flir Photon 320 thermal camera. The weights of the individual components are listed in Table I. The small helicopter weighs about 4.5 kg, including batteries, and is able to lift up a payload of about 7 kg. This capacity allows for multiple functional modules installed simultaneously, such as Ibeo and GPS/IMU forming a LIDAR system.

The Ibeo Lux laser scanner was employed to construct the mini-UAV-borne LIDAR for test. Ibeo receives echoes from four layers with angles of 0.8° synchronously, and theoretically can receive up to 38 000 points/s if only one return per pulse per layer is assumed. In practice, the nadir-looking scanner is able to record up to three returns per pulse, allowing it to get hits from ground or building walls, even covered by nearby trees. Its distance measurement range is from 0.3 to 200 m (50 m for targets with 10% remission), its accuracy is 10 cm, its angular resolution is 0.25°, and the transversal divergence of collimated beams is 0.08° with respect to the mini-UAV body [13]. The specifications of Ibeo are listed in Table II.

B. Experiment

A test flight was deployed in Vanttila, Espoo, Finland, on October 2, 2009, and the point cloud obtained in this experiment after direct georeferencing of laser range data, which is shown in Fig. 2, was employed as the mini-UAV-borne LIDAR test data. The flights were run under manual control, and

TABLE II
SPECIFICATIONS OF THE IBEO LASER SCANNER

Item	Description
Mechanism	Pulse-echo
Sampling mode	Nadir scanning
25m-longitudinal spot size (cm)	4
25m-transversal spot size (cm)	35

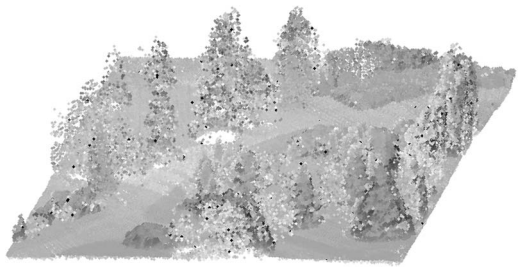

Fig. 2. Local test data acquired by Sensei LIDAR. Aside from the 3-D spatial locations, the gray scales of points refer to different intensity levels. After artificial interpretation, trees and roads have different characteristics.

therefore, the flying route and altitude were not as systematic as in typical ALS-based data collection. In addition, no strip adjustment or any other forms of registration was done to fuse the separate flights. The flying altitude above ground varied between 10 and 40 m, and the point density ranged from 100 to 1500 points per square meter for those well-covered areas. The received points comprise the coordinate triple information and are also tagged with auxiliary variables, i.e., intensity and echo species.

III. METHODOLOGY AND APPLICATIONS

The point cloud postprocessing methodologies aiming at the mini-UAV-borne LIDARs are indeed involved in various topics, e.g., point filtering or object modeling. From the perspective of mini-UAV as reference data supplier, some typical applications will be discussed with respect to its specialties of fine scale and multivariables compared to traditional LIDARs. Therefore, the next four issues are tackled to demonstrate the necessity and feasibility of mini-UAV-borne LIDAR development.

A. Tree Height Estimation

One important branch of applying LIDAR is to delineate single trees in LIDAR point clouds for retrieving tree height and other biophysical, and even biochemical, parameters. However, most previous works show that tree heights tend to be underestimated in the LIDAR-mapping mode due to a large probability of treetop missing even with a high point-sampling density [14], [15]. The fine-scale data mapped by mini-UAV-borne LIDAR can solve this issue to some extent. As compared in Fig. 3, tree heights are better represented by the collections of mini-UAV-borne LIDARs than the traditional ones, which are simulated by subsampling the real-measured data according to the reasonable density of 4 points/m^2 for the airborne LIDARs. With mini-UAV-acquired data as reference plots, the relationships of tree

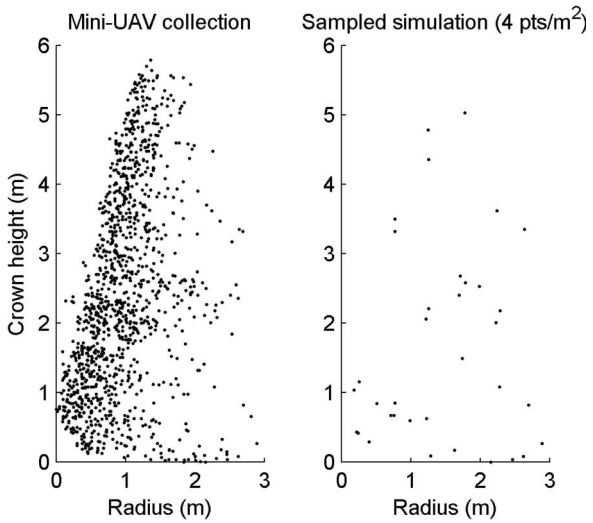

Fig. 3. Comparison of tree height representations by mini-UAV-borne LIDARs and traditional airborne ones. The traditional measurements are simulated by subsampling the real-measured data in this study, and the rule is to seek the point closer to the center of each regular grid of 0.5 m × 0.5 m. The associated height is 0.6 m less than the near real one characterized by mini-UAV data.

heights estimated in the two surveying modes can further be derived by statistics for extensive result corrections.

Automatic grouping of points into isolated trees is necessary as the premise for fulfilling tree height estimation in efficiency. The traditional tree segmentation methods based on LIDARs, e.g., the canopy surface model (CSM)-based algorithm [16], may be of low performances when applied on mini-UAV-borne LIDAR data. Other than time consumption, the irregular fluctuations of canopy surfaces tend to make crown edges drawn with errors, particularly for the deciduous trees. A multiscaled rasterization schematic is proposed in this study to improve the efficiency, and rasterization here is to seek the highest point within each raster. The coarse-scaled CSM, e.g., with a knowledge-allowed resolution of 1 m, is first generated and segmented based on the existing methods, e.g., [15] and [16], and then, the fine-scaled local CSMs associated with the temporary edges, e.g., further with a resolution of 0.1 m, are built to refine the crown boundaries. After all individual trees are determined, their heights can be predicted by subtracting the DTM produced in Section III-D from the maximum altitudes within each tree. The multiscaled rasterization method can serve as a novel solution for processing point clouds with high density, since less attention was paid in traditional LIDAR-based tree parameter retrieval.

B. Pole Detection

The altitudes of airborne laser scanners are usually between several hundred meters and few kilometers. The relatively low point density (1–20 points/m^2) and downward viewing angle make the detection of polelike objects difficult. Research [17] found that, from 400-m flight altitude (resulting in about 10 points/m^2), I-, Γ-, and T-shaped lamp poles can be extracted well (detection rates of 63%, 91%, and 100% individually) with a Toposys scanner having 1-mrad-wide beam. However, from 800-m altitude, the detection rates of I- and Γ-shaped lamps

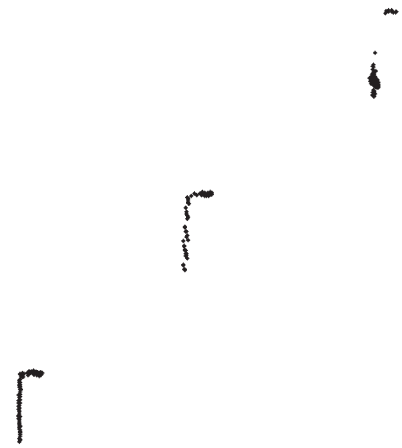

Fig. 4. Demonstration of the extracted poles from mini-UAV-borne LIDAR data. The interval and height of poles can serve as the basic geographic data. The upright pole with relatively fewer point hits is close to the edge of the scanning scene.

are greatly lower (7% and 52%). The results may be worse in engineering practice. As in Fig. 4, lamp poles are better represented by mini-UAV-borne LIDAR data as the isolated point clusters. The lighting poles are segmented by solving the gradients of the CSMs yielded during tree segmentation.

Pole detection works as the following procedure to remove the disturbances mixed in the extracted trees. Based on the CSM after tree segmentation, with a resolution of 0.05 m, the altitude gradients between the neighboring rasters beginning from the local maximum heights are calculated circle by circle expansively. Next, the steeplike gradients are sought to verify the edges of the projected poles on the ground. Sometimes, the coniferous trees with regular shapes may also have jump-type gradients within 0.1-m spacing. Thus, the local CSMs with finer scales of 0.02 m corresponding to the likely areas are acquired, and the detailed gradients are calculated. The poles can finally be confirmed. The extracted results can give the shapes of poles clearly and also reveal the distribution of pole sequences. This geographic information can be used as reference to supplement pole models often missed during traditional airborne LIDAR data processing.

C. Intensity-Based Road Extraction

Coordinate-based schematics cannot solely tackle all object detection issues, e.g., road surfaces and the surroundings having the same altitude during road extraction. Intensity then works as a key supplementary indicator to distinguish roads, and associated studies have been carried out, e.g., in [18], in which less than 80% quality with a point density of 1 point per 1.3 m^2 was achieved. The problem is that the resulted roads are still in line morphologies and cannot provide more geographic details. The mini-UAV-borne LIDARs with high point-sampling density, however, can construct fine-scale road models.

The intensity and coordinate combined schematic is assumed for road extraction, and the procedures are similarly based on the coarse-to-fine plan in Section III-A. The hybrid criteria of intensity threshold values and local altitude variations are used to verify the points belonging to roads. As shown in Fig. 5, the outlines of the targeted roads can be drawn clearly by

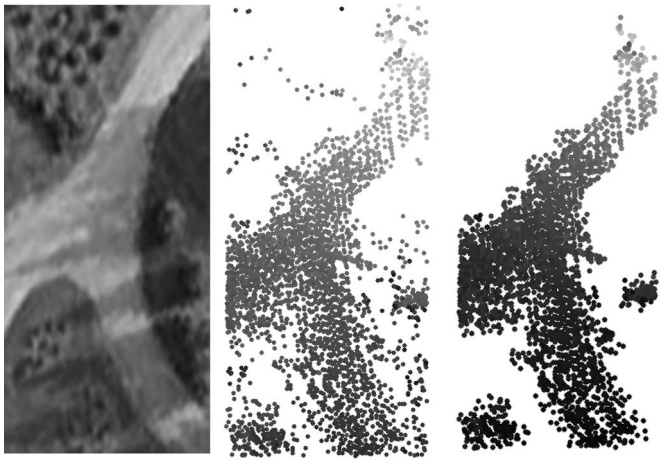

Fig. 5. Results of road extraction (middle) simply by intensity thresholding and (right) by the intensity and coordinate combined schematic. The picture (left) is the corresponding aerial image of the test area (2010 Microsoft Corporation; 2010 Blom).

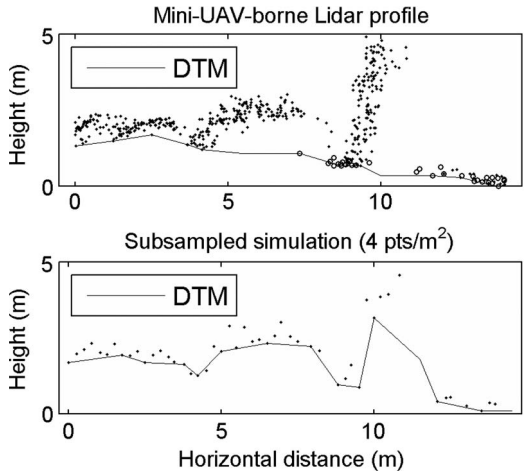

Fig. 6. Comparison of DTM extractions from mini-UAV-borne LIDAR data and traditional airborne LIDAR data, which is simulated by subsampling the real-measured data in this study. The mark "o" indicates the second or third echo per pulse. The multiecho-considered result approximates the real distribution more.

the extracted points, and the result is a good representation of the road acquired by an aerial imaging camera. Intensity calibration can further enhance the accuracy of road extraction. However, accurately extracting road edges cannot be perfectly solved just by adding the variable of intensity into LIDAR data processing. The two plots have the same intensity and altitude properties with roads, and more techniques, e.g., morphology-based method, are needed to remove the disturbances. Thus, integrating high-resolution imaging camera or other categories of sensors into the mini-UAV-borne mapping system is the following plan.

D. Multiecho-Based DTM Refinement

DTM is essential for various applications, and airborne laser scanning is an edge-cutting technique for yielding DTMs. The previous contributions on airborne laser scanner data filtering have been summarized in Sithole's dissertation [19]. However, the sparser points judged as the hits on ground from traditional LIDAR data of several points/m^2 tend to make the generated DTMs in large scales. For the high sampling density of mini-UAV-borne LIDAR, particularly with its capability of multi-echo receiving, DTMs can be produced in fine scales. Ibeo is able to record up to three returns per pulse, and in most cases, the third echoes are reflected from ground. This property can be utilized to identify the points on ground, and the altitude fluctuations of the dense points collected by mini-UAVs can also be explored to remove trees.

The concrete algorithm is to attribute different echoes with different influencing radii during vertical fragmentation for searching the lowest points. The second and particularly third echoes are given the capability of covering multisegments, and the theoretical fundamental lies in the fact that the second and third echoes mostly exist beneath trees, with crowns commonly sheltering several fragments. For example, the width of segment is set to 1 m, and the covered radius of the third echoes is valued with 4 m. If there are no points lower than the second or third echoes in the neighboring segments, the related altitude will be given to these fragments as the DTM value. The morphological filtering process based on vertical fragmenting and minimum searching can be deduced to

$$H^{Q}_{\min}\left(P^{J}_{K}\right) = \min\left(h_{P^{j}_{k}}\right) \left| \left\{P^{j}_{k}\right\}^{1,2,3}_{N} \in S_Q \right. \tag{1}$$

and if the lowest points are the second or third echoes

$$H^{Q\pm t}_{\min} = H^{Q}_{\min}\left(P^{(2|3)}_{K}\right), \qquad \text{if } H^{Q\pm t}_{\min} > H^{Q}_{\min}\left(P^{(2|3)}_{K}\right) \tag{2}$$

where the superscript j marks the echo type and the subscript k indicates the point number in the Qth fragment. The DTM value of each segment is attributed with the relative minimum altitude. Further demonstrated in (2), if the minimum height corresponds to the second or third echo, the DTM values of the neighboring fragments within the range of radius t are compared with the current minimum altitude. The DTM values of these fragments will be replaced if the previous values are larger. With a section of mini-UAV-borne LIDAR profile as the basic data, the associated DTM is generated as shown in Fig. 6, which is compared with the subsampled simulation of airborne LIDAR. The performance of multiecho-based DTM refinement is manifested explicitly.

IV. Discussions and Conclusion

In terms of all the promising results of different applications mentioned earlier, the applicability of mini-UAV-borne LIDAR for fine-scale mapping has been testified. The significances of developing this technique are embodied by, e.g., more accurate tree models, more integral pole morphologies, more applicable information for road extraction, and more definite variables for DTM refinement. As the pioneered study on mini-UAV-borne LIDAR development, the promising gains may confirm the peer researchers to work on this topic.

The mini-UAV-borne Sensei LIDAR has so many advantages. Aside from low cost and high mobility, the system can supply local reference data with high spatial resolution to revise

or calibrate traditional airborne LIDAR data or can investigate the plots of interest thoroughly as a means of in-field measurement. Moreover, it is appropriate to collect the high-temporal-resolution data efficiently for, e.g., tree foliation monitoring. With no man on board, the mini-UAV-borne LIDAR is also able to implement some dangerous tasks, such as in floods.

The merits of Sensei are not restricted in the aforementioned aspects. The system can be installed on the top of any car, and form an MLS system instantly. The specifications of all modules are simultaneously proper for terrestrial surveying [6], [7]. In addition to other instruments, e.g., camera, integrated with laser scanner, the fusion of the top-view point clouds collected by the mini-UAV-borne LIDAR and the side-view data measured with the same LIDAR on vehicle is an important research topic in the future.

REFERENCES

[1] S. Filin and N. Pfeifer, "Segmentation of airborne laser scanning data using a slope adaptive neighborhood," *ISPRS J. Photogramm. Remote Sens.*, vol. 60, no. 2, pp. 71–80, Apr. 2006.

[2] S. Solberg, E. Næsset, K. H. Hanssen, and E. Christiansen, "Mapping defoliation during a severe insect attack on Scots pine using airborne laser scanning," *Remote Sens. Environ.*, vol. 102, no. 3/4, pp. 364–376, Jun. 2006.

[3] K. Zhao, S. Popescu, and R. Nelson, "LIDAR remote sensing of forest biomass: A scale-invariant estimation approach using airborne lasers," *Remote Sens. Environ.*, vol. 113, no. 1, pp. 182–196, Jan. 2009.

[4] F. Morsdorf, C. Nichol, T. Malthus, and I. H. Woodhouse, "Assessing forest structural and physiological information content of multi-spectral LIDAR waveforms by radiative transfer modeling," *Remote Sens. Environ.*, vol. 113, no. 10, pp. 2152–2163, Oct. 2009.

[5] E. Næsset, "Accuracy of forest inventory using airborne laser-scanning: Evaluating the first Nordic full-scale operational project," *Scand. J. Forest Res.*, vol. 19, no. 6, pp. 554–557, Dec. 2004.

[6] Y. Lin and J. Hyyppä, "k-segments based geometric modeling of VLS scan lines," *IEEE Geosci. Remote Sens. Lett.*, vol. 8, no. 1, pp. 93–97, Jan. 2011.

[7] Y. Lin, A. Jaakkola, J. Hyyppä, and H. Kaartinen, "From TLS to VLS: Biomass estimation at individual tree level," *Remote Sens.*, vol. 2, no. 8, pp. 1864–1879, Jul. 2010.

[8] P. Johnson, "Unmanned aerial vehicle as the platform for lightweight laser sensing to produce sub-meter accuracy terrain maps for less than $\$5/\mathrm{km}^2$," Mech. Eng. Dept., Columbia Univ., New York, 2006.

[9] M. Nagai, T. Chen, R. Shibasaki, H. Kumagai, and A. Ahmed, "UAV-borne 3-D mapping system by multisensor integration," *IEEE Trans. Geosci. Remote Sens.*, vol. 47, no. 3, pp. 701–708, Mar. 2009.

[10] X. Zhao, J. Liu, and M. Tan, "A remote aerial robot for topographic survey," in *Proc. IEEE Int. Conf. Intell. Robots Syst.*, 2006, pp. 3143–3148.

[11] J. Geske, M. MacDougal, R. Stahl, and D. R. Snyder, "Miniature laser rangefinders and laser altimeters," in *Proc. IEEE Conf. Avionics Fiber-Opt. Photon. Technol.*, 2008, pp. 53–54.

[12] K. Lambers, H. Eisenbeiss, M. Sauerbier, D. Kupferschmidt, T. Gaisecker, S. Sotoodeh, and T. Hanusch, "Combining photogrammetry and laser scanning for the recording and modeling of the Late Intermediate Period site of Pinchango Alto, Palpa, Peru," *J. Archaeol. Sci.*, vol. 34, no. 10, pp. 1702–1712, Oct. 2007.

[13] *Ibeo Lux Laserscanner Operating Manual*, Ibeo Automobile Sensor GmbH, Hamburg, 2008, (Accessed March 2, 2010).

[14] X. Yu, J. Hyyppä, H. Kaartinen, and M. Maltamo, "Automatic detection of harvested trees and determination of forest growth using airborne laser scanning," *Remote Sens. Environ.*, vol. 90, no. 4, pp. 451–462, Apr. 2004.

[15] Q. Chen, D. Baldocchi, P. Gong, and M. Kelly, "Isolating individual trees in a savanna woodland using small footprint LIDAR data," *Photogramm. Eng. Remote Sens.*, vol. 72, no. 8, pp. 923–932, Aug. 2006.

[16] S. Solberg, E. Naesset, and O. M. Bollandsas, "Single tree segmentation using airborne laser scanner data in a structurally heterogeneous spruce forest," *Photogramm. Eng. Remote Sens.*, vol. 72, no. 12, pp. 1369–1378, Dec. 2006.

[17] E. Ahokas, H. Kaartinen, L. Matikainen, J. Hyyppä, and H. Hyyppä, "Accuracy of high-pulse-rate laser scanners for digital target models," in *Proc. 21st EARSeL Symp. Observing Our Environ. From Space: New Solutions New Millennium*, 2002, pp. 175–178.

[18] S. Clode, P. J. Kootsookos, and F. Rottensteinner, "The automatic extraction of roads from LIDAR data," in *Proc. ISPRS 20th Annu. Congr.*, 2004, vol. 35, pp. 231–236.

[19] G. Sithole, *Segmentation and Classification of Airborne Laser Scanner Data*. Delft, The Netherlands: Netherlands Geodetic Comm., 2005, pp. 9–31.